

Magnetic Propulsion of Self-assembled Colloidal Carpets: Efficient Cargo Transport via a Conveyor Belt Effect

Fernando Martinez-Pedrero¹ and Pietro Tierno^{1,2*}

¹*Estructura i Constituents de la Matèria, Universitat de Barcelona, 08028 Barcelona, Spain.*

²*Institut de Nanociència i Nanotecnologia, IN²UB, Universitat de Barcelona, Barcelona, Spain.*

(Dated: January 6, 2016)

We demonstrate a general method to assemble and propel highly maneuverable colloidal carpets which can be steered via remote control in any direction of the plane. These colloidal micropropellers are composed by ensemble of spinning rotors, and can be readily used to entrap, transport and release biological cargos on command via an hydrodynamic conveyor-belt effect. An efficient control of the cargo transportation combined with remarkable "healing" ability to surpass obstacles, demonstrate a great potential towards development of multifunctional smart devices at the microscale.

Dynamic self-assembly processes are widespread in physical systems, and occur under out-of-equilibrium conditions when for example, a driving field supplies energy and sustains a complex and otherwise unstable structure. [1] This powerful technique enables self-assembled systems adapting their environment or performing functional and sometimes programmable tasks. Examples at the microscale are disparate, including coherent patterns from ensemble of driven [2–5] or active [6–9] systems.

Time-dependent magnetic fields applied to polarizable particles represent a convenient way to assemble and propel microscopic matter in a fluid medium, since these fields do not affect the dispersing medium or alter biological systems unless the latter contain magnetic parts. The fabrication of magnetically driven artificial propellers is a research field of growing interest due to its direct application in biomedicine [10–12], targeted drug delivery [13], and microfluidics. [14]. In addition, practical applications often require the use of micromachines capable to load or unload a defined cargo on command, or to transport the latter in a defined place of a microfluidic platform or a biological network. In this context, magnetic prototypes of various form and shape have been realized so far by using DNA linked magnetic colloidal particles [15, 16], helical structures [17, 18] or other types of hybrid systems [19–21]. Besides few recent examples [16, 22], propelling structures based on pure dynamic self-assembly where cooperative interactions between the composing units lead to coherent motion of the whole system are still scarce. These structures can be used to transport efficiently biochemical cargos or to assemble, to move and to disperse the individual units in different locations.

By applying suitable magnetic manipulation techniques, we experimentally demonstrate a way to manipulate and propel large ensemble of microscopic particles assembled into highly ordered and maneuverable two-dimensional carpets via time-averaged dipolar forces. These carpets can be assembled or disassembled at will, rotated or transported in any direction of the plane via magnetic

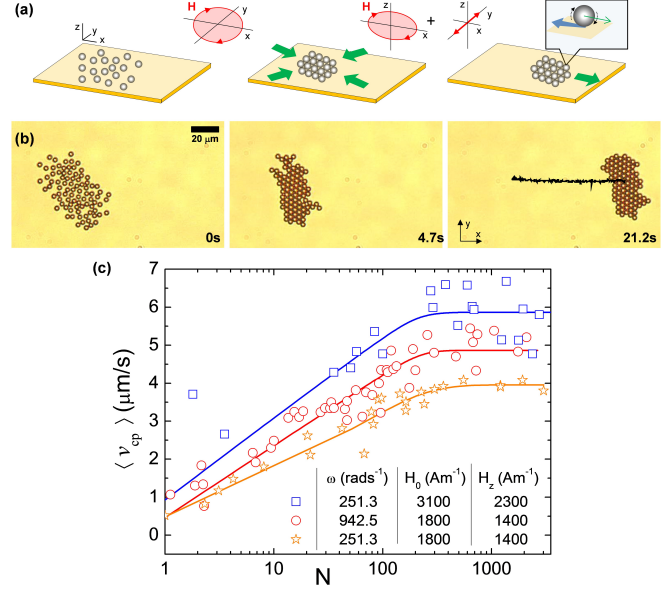


FIG. 1. Schematics showing the procedure to assemble (left-middle) and propel (middle-right) a colloidal carpet. Assembly is induced by a magnetic field rotating in the particle plane (x, y), whereas propulsion is induced by a rotating field in the perpendicular plane (x, z) plus an oscillating component along the y -axis. (b) Snapshots of a colloidal carpet assembled and propelled by an applied field with amplitudes $H_0 = 1800 Am^{-1}$, $H_z = 1400 Am^{-1}$ and frequencies $\omega = 942.5 rad s^{-1}$, $\omega_y = 471.2 rad s^{-1}$ (MovieS1 in [23]). (c) Semilog plot of the average speed $\langle v_{cp} \rangle$ versus number of particles N composing the carpet at different field values and frequencies (here, $\omega_y = \omega/2$).

control. Further we show the possibility to entrap, transport and release micro-objects such as biological cells or colloidal cargos in a fluidic environment, by using the hydrodynamic conveyor-belt generated by the moving structure. These magnetic carpets thus represent an alternative class of propelling prototypes based on dynamic self assembly.

As building blocks for the colloidal carpets we used $2.8 \mu m$ size monodisperse paramagnetic colloids (Dynabeads M-

* ptierno@ub.edu

270, Invitrogen) composed by a polymer matrix and evenly doped with superparamagnetic grains ($\sim 14\%$ iron oxide content, density $\rho = 1.3 \text{ gcm}^{-3}$). The original aqueous suspension of the particles ($\sim 7 \cdot 10^9$ beads/ml) was diluted with high deionized water ($18.2 \text{ M}\Omega \cdot \text{cm}$, MilliQ system) at a concentration of $\sim 1.4 \cdot 10^8$ beads/ml. To prevent convection effects, the colloidal suspension is sandwiched between a glass slide (Corning Incorporated) and a microscope coverslip (Agar Scientific), both separated by a double faced adhesive tape. As colloidal cargos we use either budding yeast cells (*Saccharomyces Cerevisiae*) or silica dioxide microspheres ($5 \mu\text{m}$ size, density $\rho = 2.1 \text{ gcm}^{-3}$) obtained from Sigma Aldrich.

The measurement cell is placed in the center of two orthogonal pairs of coils arranged on the stage of a light microscope (Eclipse Ni, Nikon), and aligned along the y and x axis. A fifth coil aligned along z is centered just under the sample cell. To apply time-dependent magnetic fields the coils are connected with a waveform generator (TGA1244, TTI) feeding power amplifiers (AMP-1800, AKIYAMA and BOP 20-10M, Kepco).

The paramagnetic colloids can be easily magnetized by a relatively low external field \mathbf{H} , acquiring a dipole moment $\mathbf{m} = V\chi\mathbf{H}$ pointing along the field direction. Here V is the particle volume and $\chi = 0.4$ the magnetic susceptibility under a static field. For a rotating field circularly polarized in the (x, z) plane, $\mathbf{H} = H_0(\cos(\omega t)\mathbf{e}_x - \sin(\omega t)\mathbf{e}_z)$, the particle dynamics becomes more complicated due to the presence of a finite magnetization relaxation time τ_r [24, 25]. The average magnetic torque applied to the particle can be calculated as $\mathbf{T}_m = \mu_0\langle\mathbf{m} \times \mathbf{H}\rangle$, where $\mu_0 = 4\pi \cdot 10^{-7} \text{ Hm}^{-1}$ and $\langle\ldots\rangle$ denotes a time average. Solving the relaxation equation for the magnetic moment [26] we find that, $\mathbf{T}_m = \frac{\mu_0 V \chi H_0^2 \tau_r \omega}{1 + \tau_r^2 \omega^2} \mathbf{e}_y$, where $\tau_r \sim 10^{-4} \text{ s}$ from independent measurements (data not shown). The applied torque forces the particle to rotate at an average angular velocity Ω in the fluid medium. Upon balancing \mathbf{T}_m with the viscous torque arising from the rotation in the medium $\mathbf{T}_v = -8\pi\eta\Omega a^3$ the average rotational speed reads as $\langle\Omega\rangle = \mu_0 H_0^2 \chi \tau_r \omega / 6\eta(1 + \tau_r^2 \omega^2)$. Here $\eta = 10^{-3} \text{ Pa} \cdot \text{s}$ denotes the dynamic viscosity of water.

Pair of rotors also interact via dipolar forces. The interaction potential between two equal dipoles (i, j) , at a distance \mathbf{r} away, is given by $U_{dd} = \frac{\mu_0}{4\pi} \left(\frac{\mathbf{m}_i \mathbf{m}_j}{r^3} - \frac{3(\mathbf{m}_i \cdot \mathbf{r})(\mathbf{m}_j \cdot \mathbf{r})}{r^5} \right)$, and is maximally attractive (repulsive) for particles with magnetic moments parallel (normal) to \mathbf{r} . Time averaging U_{dd} for a rotating magnetic field in the (x, y) plane gives an effective attractive potential in this plane $\langle U_{dd} \rangle = -\frac{\mu_0 m^2}{8\pi(x+y)^3}$. This interaction potential can be thus used to magnetically assemble highly ordered 2D particle monolayers [27, 28].

Fig.1(a) shows the general procedure to realize and to propel a magnetic carpet. First compact clusters are realized by applying an external uniform magnetic field circularly polarized in the (x, y) plane parallel to the glass surface, $\mathbf{H} \equiv H_0(\cos(\omega t)\mathbf{e}_x - \sin(\omega t)\mathbf{e}_y)$, being ω the

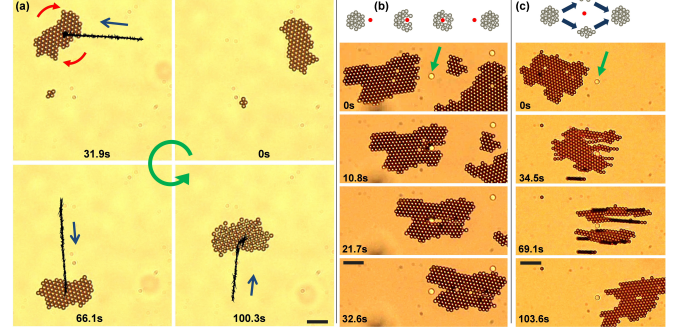


FIG. 2. (Color online)(a) Snapshots in counter clockwise order, showing the guided motion of a colloidal carpet under dynamic magnetic fields with $H_0 = 2300 \text{ Am}^{-1}$, $H_z = 1400 \text{ Am}^{-1}$ and $\omega = 942.5 \text{ rads}^{-1}$, $\omega_y = \omega/2$ (MovieS2a). Center of mass trajectory is superimposed as a black line. (b and c) Top: schematic, bottom: sequence of images of colloidal carpets moving against a $5 \mu\text{m}$ immobile silica particle. In (b) the field parameters remained constant ($H_z = 1400 \text{ Am}^{-1}$, $H_0 = 1800 \text{ Am}^{-1}$ and frequencies $\omega = 942.5 \text{ rads}^{-1} = 2\omega_y$, MovieS2b) while in (c) the field H_y was set to zero and H_z decreased to $H_z = 560 \text{ Am}^{-1}$ after $t = 26 \text{ s}$ (MovieS2c). Later ($t = 92.8 \text{ s}$) the H_y field is restored and the carpet forms again. The scale bars in all images are $20 \mu\text{m}$.

angular frequency and H_0 the amplitude. The applied field induces dipolar interactions between the magnetic colloids which are in average attractive, and the particles rapidly assemble into a close packed cluster free of defects or vacancies. The colloidal clusters are stable only in presence of the driving field, while immediately disintegrate due to thermal fluctuations once the applied field is switched off. As reported in previous works on assembly of "magnetic holes" [29] or Janus colloids [30], we observe that when the cluster is formed, it continues to rotate but at a smaller angular frequency than that imposed by the driving field. The cluster rotation arises from an unbalanced viscous shear force experienced by the torque particles located at the edge of the cluster [30, 31]. Once the carpets are formed, propulsion is obtained by applying a rotating field in the (x, z) plane plus an additional component oscillating with angular frequency ω_y along the perpendicular direction (y). The total field is given by:

$$\mathbf{H} \equiv H_0(\cos(\omega t)\mathbf{e}_x + \sin(\omega_y t)\mathbf{e}_y - \frac{H_z}{H_0} \sin(\omega t)\mathbf{e}_z), \quad (1)$$

as depicted in the right part of Fig.1(a). In most of the experiments reported here we used $H_0 \equiv H_x = H_y$ and $\omega_y = \frac{\omega}{2}$. The rotating field in the (x, z) plane exerts a torque on the individual particles forcing them to rotate close to the glass substrate. The particles acquire a net translational motion with an average speed $\langle v_x \rangle \sim \Omega a$, due to the hydrodynamic coupling with the substrate [32], making possible the propulsion of the whole carpets. The H_y component helps to keep the structure compact during motion, avoiding lateral

separation of the constituent particles. The choice of $\omega_y = \omega/2$ avoids the carpet rotation, which otherwise would occur by simply setting $\omega_y = \omega$. Fig.1(b) shows a carpet propelling with an average speed of $\langle v_{cp} \rangle = 2.7 \mu\text{m s}^{-1}$ along the x direction, keeping its structure intact. During motion the carpet trajectory is quite stable, presenting negligible displacements in the perpendicular direction. We note that in contrast to the assembly stage, the rotating field in the (x, z) plane is now strongly elliptically polarized ($H_0 \gg H_z$) in order to maintain the structure confined to two dimensions. Although the speed acquired by an individual particle (rotor) moving close to the substrate is relatively slow, for an ensemble of rotors forming the carpet the effect becomes cooperative resulting in a faster translational motion. In Fig.1(c) this effect is reflected by measuring the average propulsion speed $\langle v_{cp} \rangle$ as a function of the number of rotors N for a series of carpets having approximately a spherical shape. The continuous dashed lines are averaged curves from the experimental data showing the general trend. While $\langle v_{cp} \rangle$ initially rapidly increases with N , it saturates around $N \sim 300$, corresponding to a carpet area $S \sim 1800 \mu\text{m}^2$. Beyond this value, the rotors composing the colloidal structure start to be far away and the cooperative effect reaches its maximum efficiency. Further, we observe that at parity of frequency, increasing the field amplitude H_0 (orange stars and blue squares in Fig.1(c)) raises the average speed since the magnetic particles are subjected to higher magnetic torque and acquire a faster rotational motion. On the other hand, the propulsion speed can be also increased via the driving frequency (orange stars and red circles in Fig.1(c)), although this effect is less pronounced.

The maneuverability of our colloidal structures is shown in Fig.2(a), where the carpet is dynamically guided respectively towards the left, south and north of the observation area. As shown in MovieS2a, these turns are achieved by temporary stopping the propulsion ($H_z = 0$) and inducing a rotational motion of the carpet by setting $\omega_y = \omega = 942.5 \text{ rad s}^{-1}$. The change in direction is then obtained by restoring the field but exchanging the phases and frequencies of H_x and H_y . In Figs2(b,c) we explore the stability of the propelling carpets by forcing them to move against an immobile obstacle. As obstacle, we use a $5 \mu\text{m}$ silica particle which was permanently attached to the substrate. Fig.2b (MovieS2b) shows the carpet dynamics without changing the applied field. In this case the obstacle locally melts the moving crystal of rotors, but strong attractive dipolar interactions prevent its disaggregation, favoring re-crystallization templated by the ordered particles surrounding the melted region. An alternative method to pass the obstacle is presented in Fig.2c (MovieS2c), which could be adopted to surpass larger obstacles. In this particular situation, we split the carpet into several pieces by setting temporary $H_y = 0$ and decreasing the perpendicular field H_z . The absence of the H_y component makes the structure

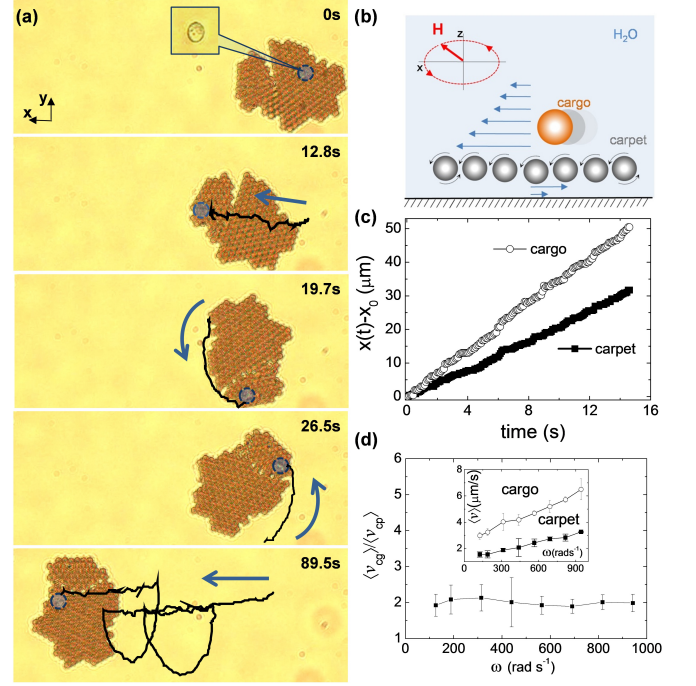


FIG. 3. (Color online) (a) Sequence of images showing the transport one yeast cell by combining translation and rotation of the carpet (MovieS3a). The position of the tracked cell is superimposed as a black line. The applied field parameters used to translate the carpet is the same as in Fig.2a. (b) Schematic of the hydrodynamic conveyor belt generated by the carpet to transport a colloidal cargo. (c) Plots of the distance versus time for the carpet (filled squares) and cargo (empty circles) for Fig3(a) from $t = 26.5\text{s}$ to $t = 41.0\text{s}$. (d) Average speed of a colloidal cargo $\langle v_{cg} \rangle$ scaled with the carpet speed $\langle v_{cp} \rangle$ as a function of ω ($H_z = 1400 \text{ Am}^{-1}$, $H_0 = 1800 \text{ Am}^{-1}$ and $\omega = 2\omega_y$). Inset shows $\langle v_{cp} \rangle$ and $\langle v_{cg} \rangle$ separately.

less stable during its propulsion, inducing the lateral separation of the constituent particles preferentially along the crystalline axis as triggered by the obstacle. After crossing the obstacle, all pieces can be reassembled back by restoring the field parameters. We note that the splitting of the carpet into pieces leads to a final different colloidal structure. Nevertheless we find that in both cases (Fig.2b and Fig.2c) the carpet is able to heal small wounds and to adapt its shape to the most compact structure after crossing the obstacle.

Non invasive approaches based on propulsive colloids to move and displace micro-objects have been achieved in the past by using elongated nanorods [33], anisotropic particles [34], helical [35] or other composite structures [36, 37]. Our self-assembled carpet allows to manipulate and transport microscopic cargos over its extended area without requirement of direct contact or chemical binding. This feature is demonstrated in Fig.3(a), corresponding MovieS3a, where a carpet having an area of $S \sim 1200 \mu\text{m}^2$ is used to transport one yeast

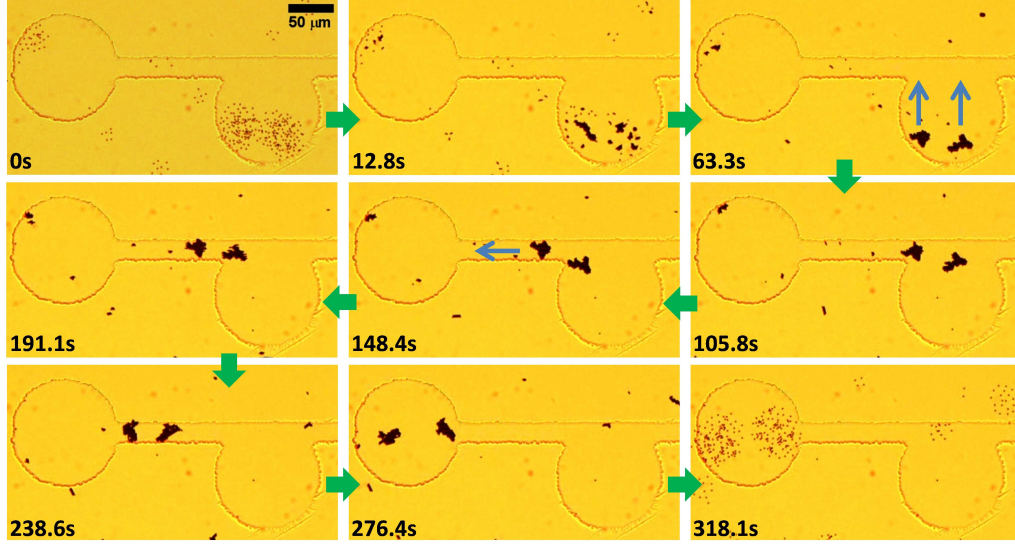


FIG. 4. (Color online) Sequence of images showing the formation of two colloidal carpets from dispersed particles (top sequence) within a glass etched circular chamber ($115\mu\text{m}$ diameter). The carpets are later transported across thin microchannels $20\mu\text{m}$ width having (middle sequence) and finally the particles are redispersed by switching off the applied field 318.1s later (MovieS4). The applied field parameters during transport are $H_0 = 1900\text{Am}^{-1}$, $H_z = 980\text{Am}^{-1}$, $\omega_z = 942.5\text{Hz}$. The frequencies are $\omega_x = \omega_z/2$ and $\omega_y = \omega_z$ ($\omega_x = \omega_z$ and $\omega_y = \omega_z/2$) when the carpets move upward (leftward).

cell along a $95\mu\text{m}$ straight path. First, as shown in the Supporting videos (MovieS3b, MovieS3c), the loading of the cargo, here a biological cell, can be realized by direct entrapment (MovieS3b) or by lifting the cargo when the carpet moves/rotates close to it (MovieS3c). Once above the magnetic carpet, the microscopic cargo is transported by using the hydrodynamic flow generated by the rotating particles. As illustrated by the schematic of Fig.3(b), this flow advects the colloidal carpet acting as a conveyor belt. Surprisingly, in contrast to other techniques to displace micro-objects, we find that the cargo moves faster than the underlying structure. For instance, in the specific case of Fig.3(a), the yeast cell travels at an average speed of $\langle v_{cg} \rangle = 3.5\mu\text{ms}^{-1}$, twice larger than the speed of the carpet. This behavior is independent of the cargo nature, as shown in Fig.3(d) where we found approximately the same ratio by employing $5\mu\text{m}$ silica particles. At parity of field strength, we observe that both $\langle v_{cg} \rangle$ and $\langle v_{cp} \rangle$ increases linearly with the frequency, and their ratio keeps constant. Increasing ω increases the rotational speed of the particles and thus the hydrodynamic flux above and below the carpet. While the colloidal cargo is free to be dragged by this flux, the colloidal carpet is slower since being closer to the surface it experience a larger hydrodynamic drag [38]. Faster speed of the cargo also implies that the latter will reach the edge and leave the carpet in a finite period of time. In order to transport the cargo for a longer distance, we manipulate the carpet inducing a $\pi/2$ rotation each time the cell reaches the edge of the structure. In the particular case of Fig.3(a), two of such rotations are required to allow the yeast cell to cover the

whole observation area in 89.5s . The ability to assemble and transport colloidal carpets close to a confining surface creates many opportunities to integrate them in a microfluidic platform. As an illustrative example, in Fig.4 we assemble and guide two colloidal carpets in a microfluidic environment. We realized a $4\mu\text{m}$ depth channel structure above a glass plate by using a wet etching (HF) technique. The structure is characterized by a network of circular compartments having $115\mu\text{m}$ diameters and connected by channels $20\mu\text{m}$ wide. Free paramagnetic colloids previously collected in one circular compartment are assembled into two separate clusters having sizes of $670\mu\text{m}^2$ and $430\mu\text{m}^2$ by an external rotating field. After $t = 63.3\text{s}$, the rotating field in the perpendicular plane is used to propel and to guide these colloidal carpets along the path connecting the two chambers. Once reached the second compartment ($t = 276.4\text{s}$), switching off the applied field melts the carpets, dispersing the particles evenly within the chamber. Even if no cargo has been transported during this operation, one can use the paramagnetic colloids directly as drug delivery vectors, since their surface can be easily functionalized with chemical agents in order to bind and to transport functional molecules [39]. Besides the basic geometries shown in Fig.4, circuits having more complex patterns can be equally explored by the propelling carpets by simply adjusting on the fly, the orientation and direction of the driving field.

In conclusion we developed a simple and versatile technique to magnetically assemble and propel highly reconfigurable colloidal carpets in all direction of the plane. Although we demonstrate this method with

commercial available paramagnetic colloids, it can be easily extended to other types of recently developed particles with heterogeneous magnetic properties such as cubes [40], ellipsoids [41], Janus [42] or anisotropic [43] ones. As opposed to existing microscopic engines chemically powered or magnetically propelled, the mechanism of motion of our carpets is cooperative and based on the rectification of the hydrodynamic flow generated by each rotor close to the bounding wall. On the application side, we showed that these mobile colloidal sheets can be used to transport biological or colloidal

cargos entrapped and translated via a hydrodynamic conveyor belt effect. Finally the carpets can be also used to assemble, maneuver and disperse microscopic particles through a microfluidics network, making them suitable for fluid based microdevices.

We thank Ignacio Pagonabarraga Mora for stimulating discussions. F.M.P. and P.T. acknowledge support from the European Research Council Project No. 335040. P.T. acknowledges support from "Ramon y Cajal" Program No.RYC-2011-07605, from Mineco (FIS2013-41144-P) and AGAUR (2014SGR878).

-
- [1] G. M. Whitesides and B. Grzybowski, "Self-assembly at all scales," *Science*, **295**, 2418 (2002).
 - [2] B. A. Grzybowski, H. A. Stone, and G. M. Whitesides, "Dynamic self-assembly of magnetized, millimetre-sized objects rotating at a liquid-air interface," *Nature*, **405**, 1033 (2000).
 - [3] M. V. Sapozhnikov, Y. V. Tolmachev, I. S. Aranson, and W.-K. Kwok, "Dynamic self-assembly and patterns in electrostatically driven granular media," *Phys. Rev. Lett.*, **90**, 114301 (2003).
 - [4] A. Snezhko and I. S. Aranson, "Magnetic manipulation of self-assembled colloidal asters," *Nat. Mat.*, **10**, 698 (2011).
 - [5] J. V. I. Timonen, M. Latikka, L. Leibler, R. H. A. Ras, and O. Ikkala, "Switchable static and dynamic self-assembly of magnetic droplets on superhydrophobic surfaces," *Science*, **341**, 253 (2013).
 - [6] W. Wang, W. Duan, A. Sen, and T. E. Mallouk, "Catalytically powered dynamic assembly of rod-shaped nanomotors and passive tracer particles," *Proc. Nat. Acad. Sci. USA*, **110**, 17744 (2013).
 - [7] Ivo Buttinoni, Julian Bialké, Felix Kümmel, Hartmut Löwen, Clemens Bechinger, and Thomas Speck, "Dynamical clustering and phase separation in suspensions of self-propelled colloidal particles," *Phys. Rev. Lett.*, **110**, 238301 (2013).
 - [8] Rodrigo Soto and Ramin Golestanian, "Self-assembly of catalytically active colloidal molecules: Tailoring activity through surface chemistry," *Phys. Rev. Lett.*, **112**, 068301 (2014).
 - [9] Félix Ginot, Isaac Theurkauff, Demian Levis, Christophe Ybert, Lydéric Bocquet, Ludovic Berthier, and Cécile Cottin-Bizonne, "Nonequilibrium equation of state in suspensions of active colloids," *Phys. Rev. X*, **5**, 011004 (2015).
 - [10] S. Sudo, S. Segawa, and T. Honda, "Magnetic swimming mechanism in a viscous liquid," *J. Intel. Mat. Syst. Str.*, **17**, 729 (2006).
 - [11] S. Guo, Q. Pan, and M. B. Khamesee, "Development of a novel type of microrobot for biomedical application," *Microsyst. Technol.*, **14**, 307 (2008).
 - [12] B. J. Nelson, I. K. Kaliakatsos, and J. J. Abbott, "Microrobots for minimally invasive medicine," *Annu. Rev. Biomed. Eng.*, **12**, 55 (2010).
 - [13] S. Kim, F. Qiu, S. Kim, A. Ghanbari, C. Moon, L. Zhang, B. J. Nelson, and H. Choi, "Fabrication and characterization of magnetic microrobots for three-dimensional cell culture and targeted transportation," *Adv. Mater.*, **25**, 5863 (2013).
 - [14] S. Sanchez, A. A. Solovev, S. M. Harazim, and O. G. Schmidt, "Microbots swimming in the flowing streams of microfluidic channels," *J. Am. Chem. Soc.*, **133**, 701 (2011).
 - [15] R. Dreyfus, J. Baudry, M. L. Roper, M. Fermigier, H. A. Stone, and J. Bibette, "Microscopic artificial swimmers," *Nature*, **437**, 862 (2005).
 - [16] P. Tierno, R. Golestanian, I. Pagonabarraga, and F. Sagués, "Controlled swimming in confined fluids of magnetically actuated colloidal rotors," *Phys. Rev. Lett.*, **101**, 218304 (2008).
 - [17] L. Zhang, J. J. Abbott, L. Dong, K. E. Peyer, B. E. Kratochvil, H. Zhang, C. Bergeles, and B. J. Nelson, "Characterizing the swimming properties of artificial bacterial flagella," *Nano Lett.*, **9**, 3663 (2009).
 - [18] P. Fischer and A. Ghosh, "Magnetically actuated propulsion at low reynolds numbers: towards nanoscale control," *Nanoscale*, **3**, 557 (2011).
 - [19] O. S. Pak, W. Gao, J. Wang, and E. Lauga, "High-speed propulsion of flexible nanowire motors: theory and experiments," *Soft Matter*, **7**, 8169 (2011).
 - [20] B. J. Williams, S. V. Anand, J. Rajagopalan, and M. T. A. Saif, "A self-propelled biohybrid swimmer at low reynolds number," *Nat. Comm.*, **5**, 3081 (2014).
 - [21] T. Qiu, T.-C. Lee, A. G. Mark, K. I. Morozov, R. Münster, O. Mierka, S. Turek, A. M. Leshansky, and P. Fischer, "Swimming by reciprocal motion at low reynolds number," *Nat. Comm.*, **5**, 5119 (2014).
 - [22] A. Snezhko, M. Belkin, I. S. Aranson, and W.-K. Kwok, "Self-assembled magnetic surface swimmers," *Phys. Rev. Lett.*, **102**, 118103 (2009).
 - [23] See EPAPS Document No.xxxx for supplementary videos.
 - [24] P. Tierno, R. Muruganathan, and T. M. Fischer, "Viscoelasticity of dynamically self-assembled paramagnetic colloidal clusters," *Phys. Rev. Lett.*, **98**, 028301 (2007).
 - [25] X. J. A. Janssen, A. J. Schellekens, K. van Ommering, L. J. van Ijendoorn, and M. W. J. Prins, "Controlled torque on superparamagnetic beads for functional biosensors," *Biosensors and Bioelectronics*, **24**, 1937 (2009).
 - [26] A. Cebers and H. Kalis, "Dynamics of superparamagnetic filaments with finite magnetic relaxation time," *Eur. Phys. J. E*, **34**, 30 (2011).

- [27] N. Osterman, I. Poberaj, J. Dobnikar, D. Frenkel, P. Zitherl, and D. Babic, “Field-induced self-assembly of suspended colloidal membranes,” *Phys. Rev. Lett.*, **103**, 228301 (2009).
- [28] J. Yan, S. C. Bae, and S. Granick, “Colloidal superstructures programmed into magnetic janus particles,” *Adv. Mater.*, **27**, 874 (2015).
- [29] Jozef Černák and Geir Helgesen, “Aggregation of magnetic holes in a rotating magnetic field,” *Phys. Rev. E*, **78**, 061401 (2008).
- [30] J. Yan, S. C. Bae, and S. Granick, “Rotating crystals of magnetic janus colloids,” *Soft Matter*, **11**, 147 (2015).
- [31] J. Schwarz-Linek, C. Valeriani, A. Cacciuto, M. E. Cates, D. Marenduzzo, A. N. Morozov, and W. C. K. Poon, “Phase separation and rotor self-assembly in active particle suspensions,” *Proc. Natl. Acad. Sci. USA*, **109**, 4052 (2012).
- [32] A. J. Goldman, R. G. Cox, and H. Brenner, “Slow viscous motion of a sphere parallel to a plane wall: motion through a quiescent fluid,” *Chem. Eng. Sci.*, **22**, 637 (1967).
- [33] T. Petit, L. Zhang, K. E. Peyer, B. E. Kratochvil, and B. J. Nelson, “Selective trapping and manipulation of microscale objects using mobile microvortices,” *Nano Lett.*, **12**, 156 (2012).
- [34] J. Palacci, S. Sacanna, A. Vatchinsky, P. M. Chaikin, and D. J. Pine, “Photoactivated colloidal dockers for cargo transportation,” *J. Am. Chem. Soc.*, **135**, 15978 (2013).
- [35] S. Tottori, L. Zhang, F. Qiu, K. K. Krawczyk, A. Franco-Obregón, and B. J. Nelson, “Magnetic helical micro-machines: fabrication, controlled swimming, and cargo transport,” *Adv. Mat.*, **24**, 811 (2012).
- [36] S. Sundararajan, P. E. Lammert, A. W. Zudans, V. H. Crespi, and A. Sen, “Catalytic motors for transport of colloidal cargo,” *Nano Lett.*, **8**, 1271 (2008).
- [37] M. S. Sakar, E. B. Steager, D. H. Kim, M. J. Kim, G. J. Pappas, and V. Kumar, “Single cell manipulation using ferromagnetic composite microtransporters,” *Appl. Phys. Lett.*, **96**, 043705 (2010).
- [38] W. B. Russel, D. A. Saville, and W. R. Schowalter, *Colloidal dispersions* (Cambridge University Press, Cambridge, 1991).
- [39] L. Yao and S. Xu, “Force-induced remnant magnetization spectroscopy for specific magnetic imaging of molecules,” *Angew. Chem. Int. Ed.*, **50**, 4407 (2011).
- [40] S. Sacanna, L. Rossi, and D. J. Pine, “Magnetic click colloidal assembly,” *J. Am. Chem. Soc.*, **134**, 6112 (2012).
- [41] O. Güell, F. Sagués, and P. Tierno, “Magnetically driven janus micro-ellipsoids realized via asymmetric gathering of the magnetic charge,” *Adv. Mater.*, **23**, 3674 (2011).
- [42] I. Sinn, P. Kinnunen, S. N. Pei, R. Clarke, B. H. McNaughton, and R. Kopelman, “Magnetically uniform and tunable janus particles,” *Appl. Phys. Lett.*, **98**, 024101 (2011).
- [43] D. Zerrouki, J. Baudry, D. Pine, P. Chaikin, and J. Bibette, “Chiral colloidal clusters,” *Nature*, **455**, 380 (2008).